NASA TECHNICAL MEMORANDUM

NASA TM X-3385

NASA TM X-3385

ALTITUDE PERFORMANCE OF A LOW-NOISE-TECHNOLOGY FAN IN A TURBOFAN ENGINE WITH AND WITHOUT A SOUND SUPPRESSING NACELLE

Thomas J. Biesiadny, Rudolph E. Grey, and Mahmood Abdelwahab

Lewis Research Center
Cleveland, Ohio 44135

NATIONAL AERONAUTICS AND SPACE ADMINISTRATION • WASHINGTON, D. C. • APRIL 1976

1. Report No.	2. Government Accession No.	3. Recipient's Catalog No.
NASA TM X-3385		

4. Title and Subtitle	5. Report Date
ALTITUDE PERFORMANCE OF A LOW-NOISE-TECHNOLOGY FAN IN A TURBOFAN ENGINE WITH AND WITHOUT A SOUND SUPPRESSING NACELLE	April 1976
	6. Performing Organization Code

7. Author(s)	8. Performing Organization Report No.
Thomas J. Biesiadny, Rudolph E. Grey, and Mahmood Abdelwahab	E-8592
	10. Work Unit No. 505-05
9. Performing Organization Name and Address	11. Contract or Grant No.
Lewis Research Center National Aeronautics and Space Administration Cleveland, Ohio 44135	
	13. Type of Report and Period Covered
12. Sponsoring Agency Name and Address	Technical Memorandum
National Aeronautics and Space Administration Washington, D. C. 20546	14. Sponsoring Agency Code

15. Supplementary Notes

16. Abstract

Test variables were inlet Reynolds number index (0.2 to 0.5), flight Mach number (0.2 to 0.8), and flow distortion (tip radial and combined circumferential - tip radial patterns). Results are limited to fan bypass and overall engine performance. There were no discernible effects of Reynolds number on fan performance. Increasing flight Mach number shifted the fan operating line such that pressure ratio decreased and airflow increased. Inlet flow distortion lowered stall margin. For a Reynolds number index of 0.2 and flight Mach number of 0.54, the sound suppressing nacelle lowered fan efficiency three points and increased specific fuel consumption about 10 percent.

17. Key Words (Suggested by Author(s))	18. Distribution Statement
Turbofan engines; Noise reduction; Engine tests; Jet aircraft noise; Propulsion system performance	Unclassified - unlimited STAR Category 07 (rev)

19. Security Classif. (of this report)	20. Security Classif. (of this page)	21. No. of Pages	22. Price*
Unclassified	Unclassified	31	$3.75

* For sale by the National Technical Information Service, Springfield, Virginia 22161

ALTITUDE PERFORMANCE OF A LOW-NOISE-TECHNOLOGY FAN IN A TURBOFAN ENGINE WITH AND WITHOUT A SOUND SUPRESSING NACELLE

by Thomas J. Biesiadny, Rudolph E. Grey, and Mahmood Abdelwahab

Lewis Research Center

SUMMARY

An experimental investigation to determine the altitude performance of a low-noise-technology fan and to compare fan and engine performance with and without a sound suppressing nacelle was conducted at the Lewis Research Center. Test variables were engine-inlet Reynolds number, flight Mach number, and flow distortion. Reynolds number indexes and Mach number were varied from 0.2 to 0.5 and 0.2 to 0.8, respectively. Tip radial and combined circumferential-tip radial distortion patterns were produced using screens upstream of the engine inlet.

There were no discernible effects of Reynolds number on fan performance over the range of conditions investigated. Increasing flight Mach number had the expected effect of shifting the fan operating line such that at a given corrected fan speed, the fan pressure ratio decreased and the corrected fan airflow increased. Inlet flow distortion shifted the fan operating and stall line towards each other producing a lower stall margin.

For a Reynolds number index of 0.2 and flight Mach number of 0.54, the sound suppressing nacelle lowered the fan efficiency as much as three points and increased the specific fuel consumption of the engine about 10 percent when the pressure losses associated with the nacelle were taken into account.

INTRODUCTION

Efforts to reduce the fan noise emitted from jet engines have resulted in fan designs incorporating low noise technology, such as proper rotor-stator axial spacing and blade-vane ratio. In addition, fan inlet and exit ducting designs have embodied duct splitter rings allowing the more liberal use of sound suppression material. While these techniques have led to reduced noise levels (ref. 1), their effects on fan and engine performance need to be established.

An engine incorporating the noise technology just discussed (refs. 2 and 3) was tested in an altitude facility at the Lewis Research Center. These tests were conducted with and without a sound suppressing nacelle (ref. 4) over a range of inlet Reynolds number indexes and flight Mach numbers from 0.2 to 0.5 and 0.2 to 0.8, respectively. In addition, typical fan data were obtained with two inlet flow distortion patterns (a tip radial and a combined circumferential-tip radial) as well as with uniform inlet flow.

Test results illustrate the effects of inlet Reynolds number, flight Mach number, inlet flow distortion and a sound suppressing nacelle on the fan bypass and overall engine performance. Fan performance is described by fan maps using parameters of pressure ratio, corrected airflow and rotative speed, and efficiency. The effects of inlet Reynolds number, inlet distortion and the sound suppressing nacelle are shown at one flight Mach number (0.54) over a range of Reynolds number indexes (0.2 to 0.5). The effect of flight Mach number is presented for one Reynolds number index (0.2) over a range of Mach numbers (0.2 to 0.8). Overall engine performance is described by specific fuel consumption and net thrust. The effect of the sound suppressing nacelle on engine performance is shown for one flight Mach number (0.54) and Reynolds number index (0.2). The losses associated with the sound suppressing nacelle are also presented.

APPARATUS

Engine

The two-spool high bypass ratio (5.6) engine used in this investigation consisted of the low noise technology fan described in reference 1 and a modified CF6 core matched to the engine thrust requirement of 98 000 newtons (22 000 lb) sea level static. The engine shown schematically in figure 1(a) incorporated a single-stage 40-blade fan of 1.8 meter (6 ft) diameter with outlet guide vanes (90 blades) at a blade-vane spacing of two chords. The fan hub-tip radius ratio was 0.465 at rotor inlet. The fan was driven by a low pressure turbine modified to four stages by removing one stage from the CF6 design. The turbine was matched to the fan by closing the first-stage nozzle diaphragm 6 percent. The core engine embodied a 16-stage compressor, annular combustor, and a two-stage turbine. Fan and core streams were separate.

Sound Suppressing Nacelle

The sound suppressing nacelle used in these studies, shown schematically in figure 2, consisted of acoustically treated surfaces in both the engine inlet, shown pictori-

ally in figure 3, and the fan duct. Also shown in figure 2, immediately upstream of the inlet hardware is the transition piece used to adapt the nacelle to the uniform flow inlet ducting.

The sound suppressing configuration at the engine inlet, shown in fore and aft view in figure 3, was made of three rings of acoustic treatment along with acoustically treated outer wall and centerbody. Six forward and three aft radial struts supported both the rings and the centerbody. Also shown in the rear view is some of the fan inlet instrumentation that was unique to the sound suppressing nacelle.

Facility

Engine installation. - A photograph of the engine installation, a conventional direct connect type, in the altitude test chamber is shown in figure 4. The engine, shown with sound suppressing nacelle attached, was hung from a mounting structure which was attached to a thrust bed. The thrust bed, in turn, was suspended by four flexure rods attached to the chamber supports and was free to move except as restrained by a dual load cell system that allowed the thrust bed to be preloaded.

The chamber included a forward bulkhead which separated the inlet plenum (5. 5 m (18 ft) diam) from the test chamber (7. 3 m (24 ft) diam). Air of the desired temperature and pressure flowed from the plenum through the bellmouth to the inlet duct (fig. 1(a)). A conical screen was attached to the bellmouth to prevent foreign object ingestion. A labyrinth seal, shown schematically in figure 1(b), was used to isolate the inlet ducting from the bellmouth and bulkhead. The inlet ducting was joined to the engine through a gimbal joint which allowed freedom of movement of the engine.

Engine exhaust gases were captured by a collector which extended through the rear bulkhead thereby minimizing the possibility of exhaust gas recirculation in the test chamber.

Computer. - The facility digital computer, which monitored test parameters, acquired steady state, dynamic, and frequency inputs. These were converted to engineering units and were available for test parameter computations and real time display at the rate of once per second. Line printer output of engineering units and test parameters were available upon command. In addition to the data acquisition and reduction function, limit checks were performed by the computer and alarms displayed for limit violations, also on a once per second basis. Control parameters could also be sent to control devices.

An analog computer was also interfaced with the digital computer for averaging of critical parameters for periods longer than that normally available.

Fan Back Pressure Jets

Operation of the fan from its normal operating line to its stall or stress limit was possible by using a fan back pressure jet system (ref. 5). This system provided the capability of varying the effective fan exit area and is shown schematically and pictorially in figure 5. The hardware consisted of a manifold or accumulator supplied by high pressure air and pipes from this manifold which terminated in nozzles that uniformly directed the flow counter to the fan exit flow. The jet flow was controlled by facility valves upstream of the manifold. The back pressure jet system produced a reduced fan exit effective area because of the addition of mass flow and the reduction of fan exit flow momentum. There was no evidence that the total pressure profile at the fan exit was altered by this jet flow.

Distortion Screens

Engine inlet total pressure distortions were produced by tip radial and combined circumferential-tip radial (modified circumferential) distortion screens at the locations shown in figures 1 and 2. The screens are illustrated in figure 6. The tip radial distortion screen, figure 6(a), which covered 40 percent of fan duct annular area and had a solidity of 50 percent was used because of previous testing with this screen during a rig evaluation of the fan. The modified circumferential screen, figure 6(b), was a 180° section of the tip radial screen. This configuration was chosen because of a desire to test with a circumferential distortion which would not produce flow distortions in the core compressor. The 45° to 225° location was selected so that critical strain gage measurements on the outlet guide vanes were in the distorted region.

Instrumentation

The instrumentation identification by station and probe location is shown in figures 1 and 2 for the configuration with and without the sound suppressing nacelle (see appendix A for a list of symbols and their identity). The instrumentation was identical for the two configurations except for the fan inlet (station 2.0) and the fan nozzle (station 2.8) where acoustic treatment or the absence of it influenced the choice of instrumentation. Used only for the sound suppressing nacelle (fig. 2) were the traversing probe and the arc rakes, positions for which are also shown in figure 3(b) at the fan inlet station. Data from these instruments were used to determine the pressure defect behind the acoustic rings and support struts.

Steady-state pressures were recorded on twenty-five scanivalves (24 ports each)

operated by the facility computer and individual transducers. Chromel-Alumel thermocouples referenced to a 339 K (610° R) oven were used throughout the installation to measure temperatures. Thrust was measured by 89 000-newton (20 000-lb) load cells mounted below the thrust bed. The thrust signal, in turn, was integrated by an analog computer for 0.8 second.

High-response transducers mounted as wall statics both upstream and downstream of the fan were used as stall indicators. The downstream instrumentation failed shortly after testing began, however, and did not figure significantly in the stall investigation.

Sixteen strain gages mounted on the fan blades and outlet guide vanes were used in conjunction with the high-response transducers to determine the approach of limiting stress levels and the onset of stall.

Instrument and system accuracies along with a more detailed description of the instrumentation are presented in appendix B.

TEST PROCEDURES

Engine Conditions

Engine operating conditions were set by adjustments in the plenum and test chamber pressures to maintain flight Mach number and engine-inlet Reynolds number index. Airflow limitations in the facility equipment prevented simulation of conditions greater than a flight Mach number of 0.8 and a Reynolds number index higher than 0.5. Difficulties in stabilizing low flight Mach number test conditions limited the minimum Mach number to 0.2.

Tests with the sound suppressing nacelle were limited during the latter part of the program to Reynolds number indexes of 0.23 or greater because of oil loss above 12 800 meters (42 000 ft). A further discussion of the choice of engine inlet conditions with and without the sound suppressing nacelle can be found in appendix C, Methods of Calculation.

Fan speeds for configurations without fan back pressure jets were varied from idle to 3400 rpm.

Thrust parameters were measured, as described in appendix C, without the fan back pressure jets or the distortion screens installed.

Fan Back Pressure Jets

The fan back pressure jets were used to produce fan performance maps employing the identical procedures for configurations with and without the sound suppressing na-

celle. The fan exit pressure was slowly increased by increasing the jet pressure and therefore the flow at constant fan speed and inlet and exhaust conditions until fan stall or a stress limit was reached. During fan mapping, the core speed varied because of a rematching of the fan and core rotors.

For fan performance mapping, speeds were limited to 2900 rpm for the unsuppressed configuration, because it was considered undesirable to initiate fan back pressure at higher speeds where engine vibrations, though within limits, were high. With the sound suppressing configuration, fan speeds of 3080 rpm were possible before vibration limits were approached.

RESULTS AND DISCUSSION

Fan Performance

The performance of the fan is described in the figures 7 to 16 using parameters of pressure ratio, corrected total fan airflow, corrected rotative speed, and efficiency. The values of pressure ratio and efficiency were based on measurements in the fan bypass flow region. The stall limits of the fan were defined from either the formation of rotating stall, as indicated by high-response pressure measurements, or high stress levels, as indicated by strain gages, which experience had shown to be incipient with stall.

Uniform inlet flow. - Fan performance without the sound suppressing nacelle is presented in figure 7 for Reynolds number indexes of 0.2 and 0.5 at a flight Mach number of 0.54. There were no discernible effects of Reynolds number (within the range explored) on the operating, speed, and stall lines or the efficiency levels. As corrected fan speed was increased from 2000 to 2900 rpm, the peak efficiency levels rose from 0.750 to 0.815.

Fan performance with the sound suppressing nacelle is presented in figure 8 for Reynolds number indexes of 0.23 and 0.50 at a flight Mach number of 0.54. Again, no effect of Reynolds number was detected. With the sound suppressing nacelle, the peak fan efficiency increased from 0.740 to 0.800 as corrected fan speed was increased from 2000 to 3080 rpm.

A comparison of the data with and without the sound suppressing nacelle is shown in figure 9. The constant corrected speed line and its accompanying efficiency at 2900 rpm for the sound suppressing nacelle were obtained by interpolating the data of figure 8. The effect of the sound suppressing nacelle on the operating, speed, and stall lines showed a general shift of the operating range to lower airflows and pressure ratios. However, there was some evidence that the shift in operating line with the sound suppressing nacelle was a result of the axial position of the back pressure jet hardware in

relation to the fan nozzle exit plane. Though the shift was noticeable at the highest fan speed, it was less significant at the lower speeds.

The effect of the sound suppressing nacelle on fan efficiency was to lower the efficiency by as much as three points. This trend toward lower efficiencies might be expected inasmuch as the data presented for the sound suppressing nacelle configuration included the pressure losses associated with its inlet (see Methods of Calculation). The inlet pressure losses with the sound suppressing nacelle are shown in a subsequent figure.

In an effort to complete the comparison of the effect of the sound suppressing nacelle on the fan performance, fan efficiencies were calculated based on the pressure surveys taken downstream of the suppressing inlet. These data along with data from the unsuppressed configuration are shown in figure 10 where fan efficiency is presented as a function of corrected total fan airflow for a Reynolds number index of 0.2 and flight Mach number of 0.54.

Little or no difference existed between the two configurations at 2900 rpm. A larger difference of approximately six points, however, was evident at the lowest speed, 2000 rpm, investigated. There are several known reasons or factors that could contribute to the aforementioned trend. One of the more obvious reasons would be the lack of adequate pressure and temperature measurements at the fan inlet and exit, thereby resulting in inaccurate averages of these parameters. An examination of the measurement coverage and profiles indicated that this factor was not significant with respect to the efficiency differences with the nacelle. Another reason for this efficiency trend may be the effect of the inlet sound suppression rings and struts on the fan radial flow balance or the turbulence level.

The effect of Mach number on the fan operating line and efficiency is presented in figure 11 where pressure ratio and efficiency are plotted as a function of corrected total fan airflow. These data show that, as flight Mach number was increased at a constant corrected fan speed, the fan operating point moved to lower pressure ratios and increased corrected airflows. Fan efficiencies were maximum in the 0.3 to 0.5 Mach number range and at the lower fan speeds declined substantially as Mach number was raised above 0.5. As an example, at 2400 rpm peak efficiency of 0.735 occurred at a Mach number of approximately 0.3 but decreased to 0.635 at a Mach number of 0.8. For 3200 rpm, peak efficiency was at a Mach number of approximately 0.5 but there was no substantial drop in efficiency for higher Mach numbers. These results are influenced by the fact that the fan nozzle was not choked for any of the conditions investigated.

Inlet flow distortion. - The effect of inlet flow distortion on fan performance is shown in figures 12, 13, and 14. Presented in figure 12 are typical fan inlet total pressure profiles during flow distortion. Shown in figures 13 and 14 are fan performance data with distortion and a comparison of these results with uniform inlet flow.

Illustrated in figure 12(a) is the total pressure profile in a radial direction which

was applicable to both the tip radial and the modified circumferential distortion. Displayed in figure 12(b) is the total pressure profile in the circumferential direction for the modified circumferential distortion. Both sets of data are for corrected flow rates of approximately 372 kg/sec (820 lb/sec). At these conditions, the minimum ratio of local total pressure to the total pressure upstream of the distortion screen location was in the 0.87 to 0.91 range.

The performance data shown with distortion (figs. 13 and 14) were obtained with the sound suppressing nacelle and at a Reynolds number index of 0.23 and a flight Mach number of 0.54. Similar data taken without the nacelle and at other Reynolds number indexes but the same Mach number exhibited similar results. The effect of both distortions was to reduce the uniform inlet flow stall margin by shifting the operating and stall lines toward each other. The effect of the tip radial was somewhat more severe on stall margin than the modified circumferential. In comparing the constant speed lines, the tip radial had little or no effect. The modified circumferential distortion, however, had the effect of reducing the fan pressure ratio generated at a given corrected fan speed line.

The effect of distortion on fan efficiency was not readily apparent because of inconsistency in the trends. The tip radial distortion resulted in a higher efficiency at the lower speeds and only a slight detrimental effect at the highest speed tested. The modified circumferential distortion had little or no effect on efficiency at the lower speeds but did produce a somewhat lower efficiency at the highest speed. These trends should be considered somewhat uncertain because of the possible effects of distortion on the fan inlet and exit profiles and the relatively high sensitivity of efficiency to any measurement error.

Sound Suppressing Nacelle Pressure Losses

The sound suppressing nacelle used during this investigation had a full complement of acoustic treatment (ref. 4). Typical pressure loss in the inlet of the nacelle is presented in figure 15 where the ratio of the pressure difference across the inlet to the pressure upstream of the inlet is shown as a function of corrected total fan airflow. The pressure loss varied from about 1 to 1.5 percent over the range of corrected total fan flows tested. The predicted inlet pressure loss from reference 4 for both the takeoff and cruise (M_0 = 0.82, altitude = 10 670 m (35 000 ft)) conditions was 1.0 percent. These levels of loss then represent the penalty imposed by the acoustically treated inlet rings and their supporting struts. For comparison, the pressure loss from station 1 to station 2 with the nacelle hardware removed was negligible.

Typical pressure loss in the exit fan duct for the sound suppressing nacelle is displayed in figure 16 where the ratio of the pressure difference across the exit fan duct to

the pressure at the fan exit is shown as a function of corrected total fan airflow. The pressure loss varied from about 4 to 5 percent over the range of corrected total fan flows investigated. These data represent the loss in the exit fan duct associated with the acoustic treatment and the engine pylon from which the engine was supported. Also shown in figure 16 is a pressure loss curve that represents the loss without the nacelle. Inasmuch as both configurations required the engine pylon, the difference of the loss levels shown in this figure represent the losses attributable to the splitter and acoustic treatment on the walls only and ranged from 1.5 to 2 percent. The predicted fan duct pressure loss (ref. 4) was 1.9 percent at takeoff and 2.7 percent at cruise.

Engine Performance

Another measure of comparison illustrating the effect of the sound suppressing nacelle on performance is the overall engine performance for the two configurations. A representative comparison is presented in figure 17 where corrected specific fuel consumption is shown as a function of corrected net thrust. The equations used for the thrust determination and the related parameters are presented in appendix C. These particular data were obtained at a Reynolds number index of 0.2 and a flight Mach number of 0.54. The sound suppressing nacelle configuration exhibited a specific fuel consumption 8 to 12 percent higher than without the nacelle depending on the thrust level. The predicted increase in specific fuel consumption in reference 4 was 4.0 percent at the cruise condition.

SUMMARY OF RESULTS

An investigation was conducted to determine the altitude performance of a low-noise-technology fan and to compare fan and engine performance with and without a sound suppressing nacelle. The principal results of this investigation were:

1. A reduction in inlet Reynolds number index from 0.5 to 0.2 produced no discernible effects on fan performance with or without the sound suppressing nacelle.

2. Increasing the flight Mach number at a constant corrected fan speed resulted in a decrease in fan pressure ratio and an increase in corrected airflow.

3. Inlet flow distortion shifted the fan operating and stall line towards each other with an attendant reduction in stall margin.

4. At a Reynolds number index of 0. 2 and flight Mach number of 0. 54, the fan efficiency decreased as much as three points and the engine specific fuel consumption increased about 10 percent when the sound suppressing nacelle was utilized.

Lewis Research Center,
National Aeronautics and Space Administration,
Cleveland, Ohio, January 27, 1976,
505-05.

APPENDIX A

SYMBOLS

A	flow area, cm^2
M_0	flight Mach number
N	rotor speed, rpm
P_S	static pressure, N/cm^2
P_T	total pressure, N/cm^2
R	gas constant, J/(kg)(K)
RNI	Reynolds number index, $\delta/(\mu/\mu_{SL})\sqrt{\theta}$
R_i	inner radius, cm
R_o	outer radius, cm
r	radius, cm
SFC	specific fuel consumption, kg/(hr)(N)
T	temperature, K
V_0	flight velocity, m/sec
W	mass flow rate, kg/sec
α	angle, deg
γ	ratio of specific heats
δ	ratio of total pressure to standard sea-level static pressure
η	adiabatic efficiency
θ	ratio of total temperature to standard sea-level static temperature
μ	absolute viscosity, kg/(m)(sec)

Subscripts:

a	air
INLT	average engine inlet condition, see appendix C
F	fan
f	fuel
L	labyrinth
SL	sea level

1 airflow measuring station

2 fan inlet

2.3 fan exit

2.8 fan nozzle

APPENDIX B

INSTRUMENT ACCURACIES

Instrument calibration accuracies for the pressures, temperatures, thrust load cells, and fuel meters associated with the fan and engine performance parameters presented in this report are given here. The equations for the performance calculations can be found in appendix C.

The pressures were measured by two different devices, the scanivalve transducer for multiple pressure readings with one instrument and the individual transducer for single measurements. The scanivalve transducers, which recorded the greater portion of the data, were differential in nature with a full-scale range of ± 10.3 N/cm^2 (± 15 psi). Known reference levels were used to calibrate the transducers, the high pressure being atmosphere, the low, a vacuum level. The instrument and system accuracies associated with these scanivalve transducers were ± 0.047 N/cm^2 (± 0.068 psi). The accuracy of the individual type transducer was ± 0.014 N/cm^2 (± 0.020 psi).

The estimated accuracy for the Chromel-Alumel thermocouples used for all temperatures in the system was ± 0.554 K ($\pm 0.998^\circ$ R). At the fan exit (station 2.3) this included the individual calibration of the thermocouple rakes for ram recovery.

The thrust load and preload cells used for the engine performance parameters were 89 000 newtons (20 000 lb) full scale. Calibration curves for both load cells were accurate to within ± 0.05 percent of full scale.

Fuel flow, the other parameter used in engine performance calculations, was measured by two low range meters in series and two high range meters in series. All meters were individually calibrated. Frequency to flow conversion constants for these calibrations were accurate to within ± 0.5 percent over the linear range of each meter.

Fuel temperature, though not controlled, varied from 280 to 289 K (505° to 520° R) for the data presented.

APPENDIX C

METHODS OF CALCULATION

Inlet Reynolds Number Index and Flight Mach Number

Without the nacelle, the engine or fan inlet conditions were based on the measurements at station 2, which were essentially the same as those at station 1, the airflow measuring station. With the nacelle, the engine or fan inlet conditions were based on measurements taken at station 1, upstream of the acoustically treated inlet. The primary reason for this choice was the greater stability of test conditions based on station 1 pressures as opposed to an integrated pressure at station 2 resulting from traversing probe surveys. A secondary reason was the desire to minimize the testing with the traversing probe from safety considerations.

For distortion testing without the nacelle, the test conditions were set using pressures in the undistorted region at station 2. During distortion tests with the nacelle, test conditions were again based on the undistorted conditions. However, because station 1 was located upstream of the distortion screen and its supporting grid, the pressure loss across the grid was established using data without the nacelle. This pressure loss was a function of the total corrected airflow.

Average Inlet Temperature and Pressure

The average engine inlet temperature was assumed to be equal to the average plenum temperature for all test conditions.

The average inlet pressure without the nacelle was based on the average pressure at station 2 with and without inlet distortion present. The nacelle inlet pressure, however, was based on the average at station 1 for the uniform flow test conditions. The only exception to this was the data shown in figure 10 where fan efficiencies were calculated using integrated pressures downstream of the nacelle (station 2). With distortion present, the average inlet pressure was obtained from the pressure loss across the distortion screen and its support structure for the configuration without the nacelle.

Total Airflow

Total airflow at the engine inlet was calculated at station 1 with and without the nacelle using the following equation:

$$W_{a_1} = A_1 P_{T_1} \left[\frac{2\gamma_1}{RT_1(\gamma_1 - 1)} \right]^{1/2} \left(\frac{P_{S_1}}{P_{T_1}} \right)^{1/\gamma} \left[1 - \left(\frac{P_{S_1}}{P_{T_1}} \right)^{(\gamma_1 - 1)/\gamma_1} \right]^{1/2}$$

The average total pressure was obtained by an integration procedure which accounted for the boundary layer.

Fan Efficiency

Fan efficiency was defined as the ratio of the ideal temperature rise to the actual temperature rise. Assuming isentropic conditions, the ideal temperature rise was calculated from the actual pressure rise across the fan; that is,

$$\eta_F = \frac{\left(P_{T_{2.3}} / P_{T_{INLT}} \right)^{(\gamma - 1)/\gamma} - 1}{(T_{2.3}/T_2) - 1}$$

Engine Net and Gross Thrust

The engine net thrust was defined as

$$F_N = F_G - F_{RAM}$$

where

F_N net thrust

F_G gross thrust

F_{RAM} ram drag, $W_{a_1} V_0$

The gross thrust was defined as

$$F_G = F_M - F_p + F_{DEFL} + F_{TARE} + F_1 + F_{SEAL} - F_{EXT} - F_{FN} - F_{FP} - F_{BT}$$

where

F_M load cell measurement

F_P preload

F_{DEFL}	deflection of thrust bed plus friction in bed
F_{TARE}	drag force caused by air flowing through labyrinth seal
F_1	momentum at station 1
F_{SEAL}, F_{EXT}	forces acting on labyrinth seal flange
F_{FN}, F_{FP}, F_{BT}	forces acting on the fan nozzle, core nozzle, and pylon (see fig. 1(c)) if surface pressures were greater than test chamber pressure. These terms were found to be negligible

Specific Fuel Consumption

Specific fuel consumption was defined as

$$SFC = \frac{W_f}{F_N}$$

REFERENCES

1. Sanders, Newell D.: A Quiet Engine for Stilling Complaints. Astron. and Aeron., vol. 11, no. 1, Jan. 1973, pp. 40-48.

2. Experimental Quiet Engine Program. Volume 2, Phase I - Engine Design Report. (General Electric Co.; NAS3-12430), NASA CR-72967, 1970.

3. Kazin, S. B.; and Paas, J. E.: NASA/GE Quiet Engine A Acoustic Test Results. (GE-R73AEG363, General Electric Co.; NAS3-12430), NASA CR-121175, 1973.

4. Tucker, R. H.; et al.: Developmental Design, Fabrication, and Test of Acoustic Suppressors for Fans of High Bypass Turbofan Engines. NASA CR-2338, 1974.

5. Biesiadny, T. J.: Test Techniques for Obtaining Off-Nominal Compressor Data During Engine Tests. SAE Paper 740822, Oct. 1974.

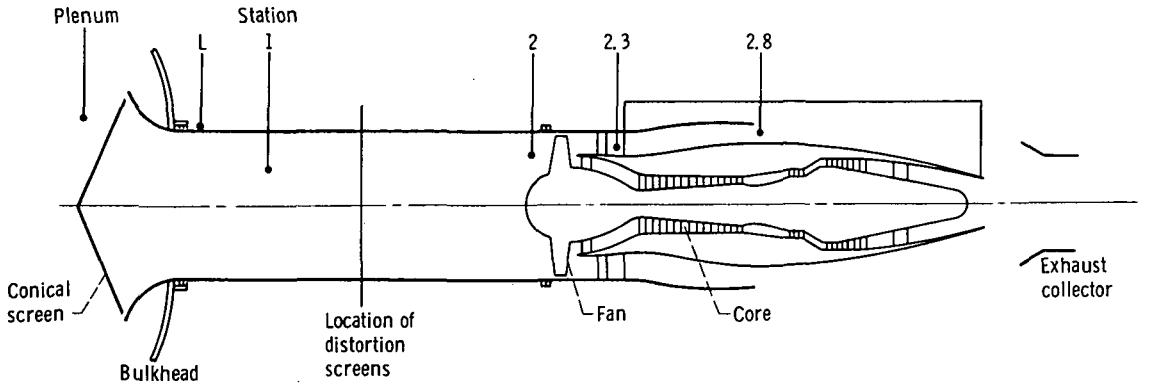

(a) Station locations.

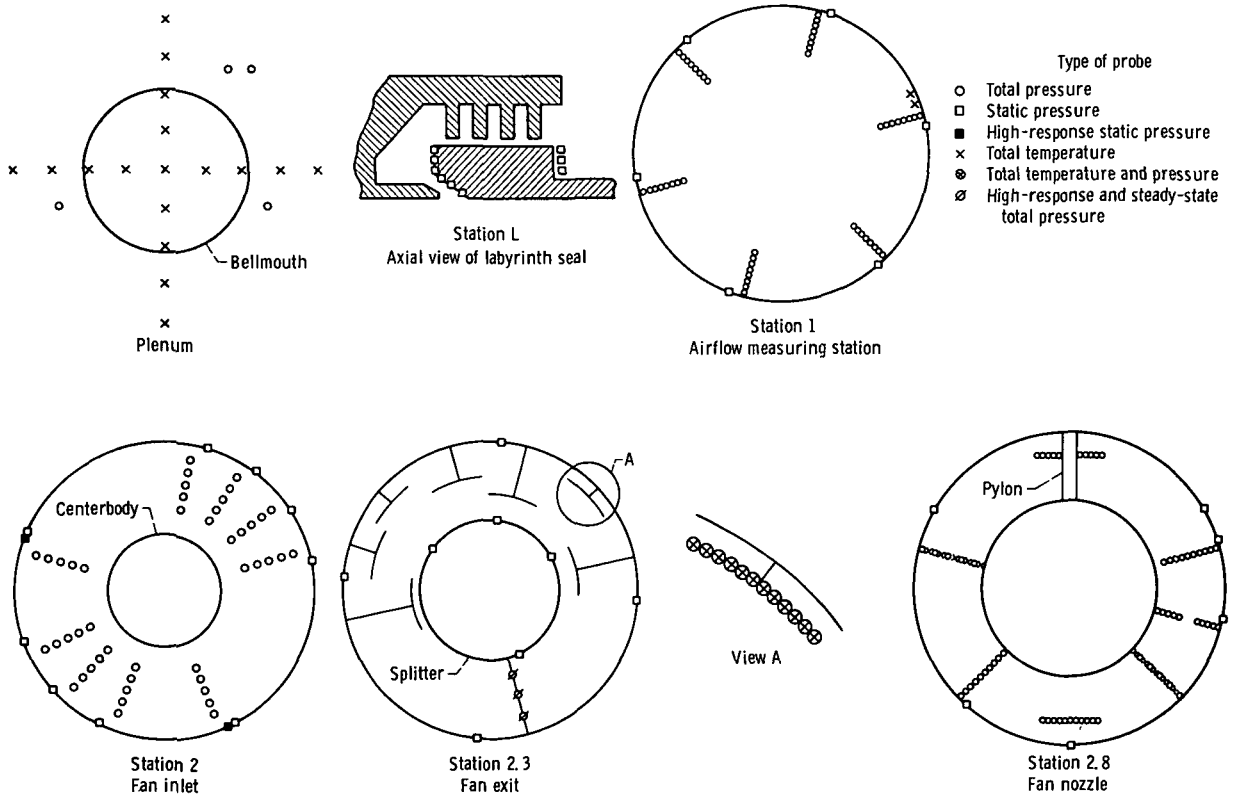

(b) Individual station layouts (instrumentation stations viewed looking upstream).

Figure 1. - Nonsuppressing configuration with instrumentation layout.

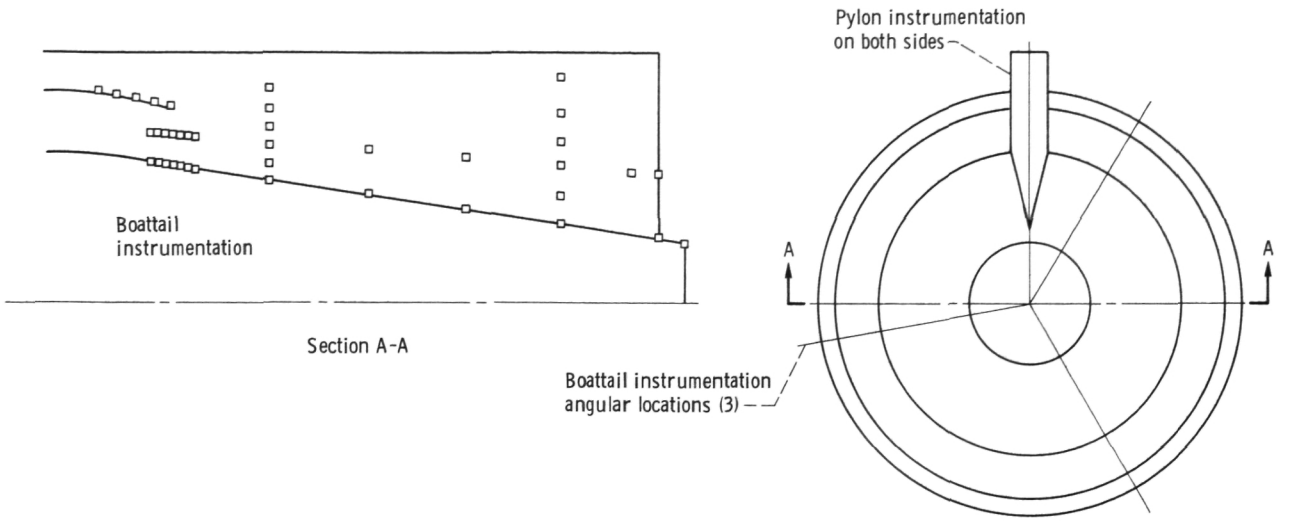

(c) Boattail and pylon statics.

Figure 1. - Concluded.

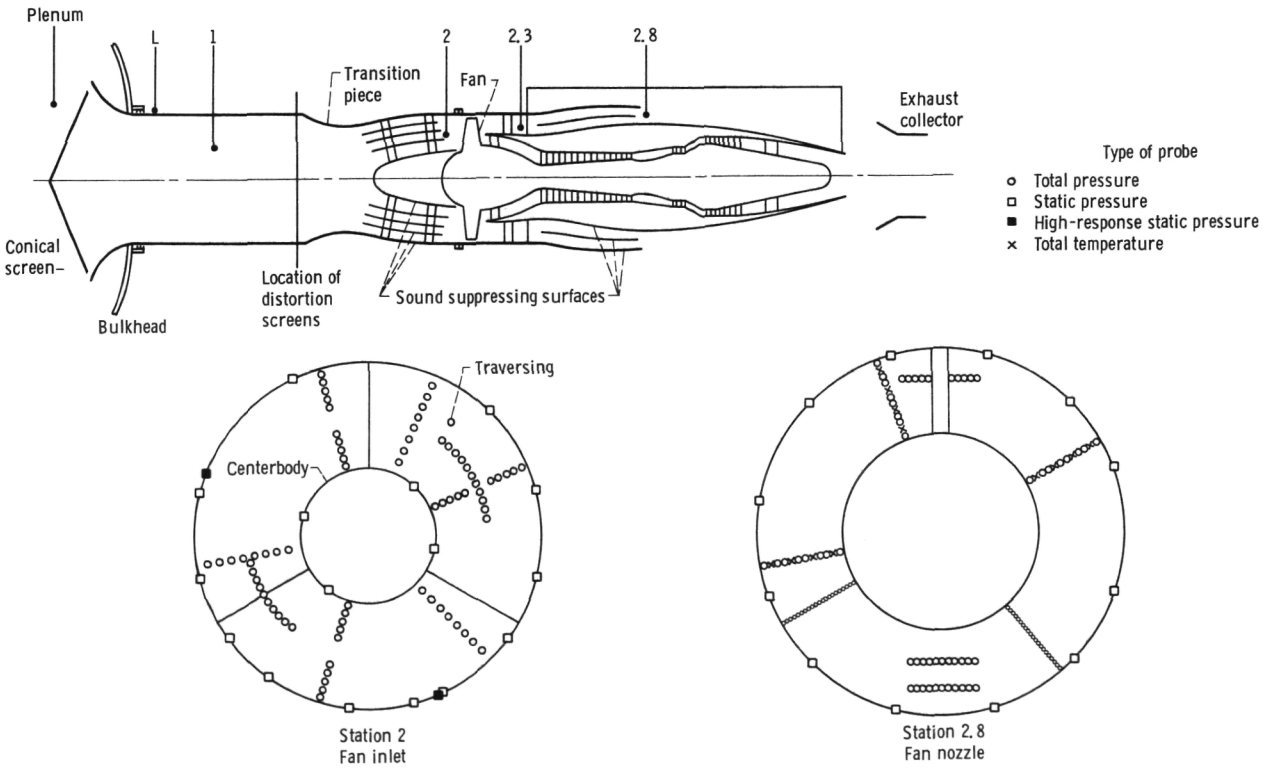

Figure 2. - Sound suppressing nacelle with instrumentation layout of modified stations (instrumentation stations viewed looking upstream).

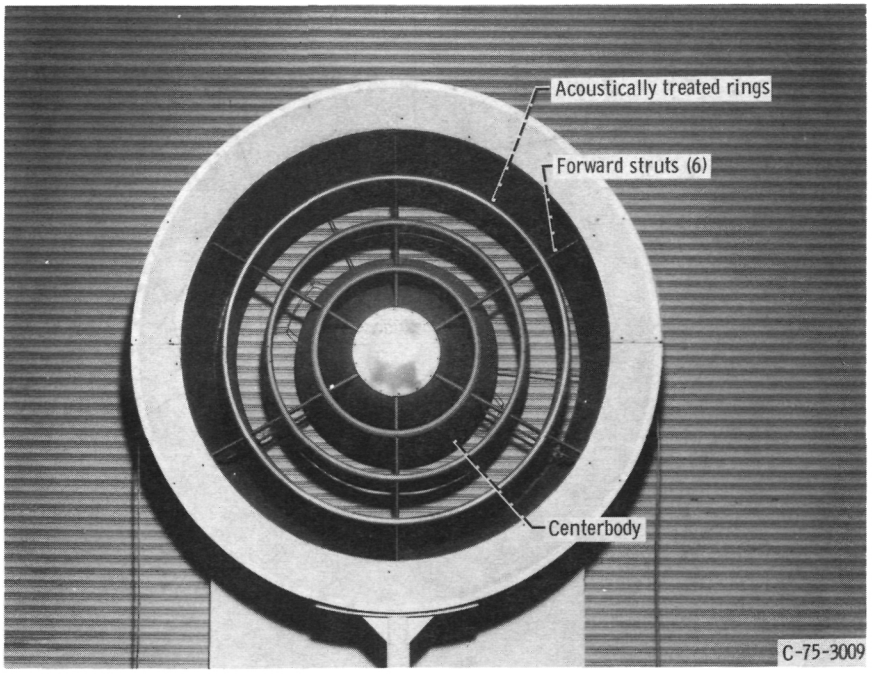

(a) Front view.

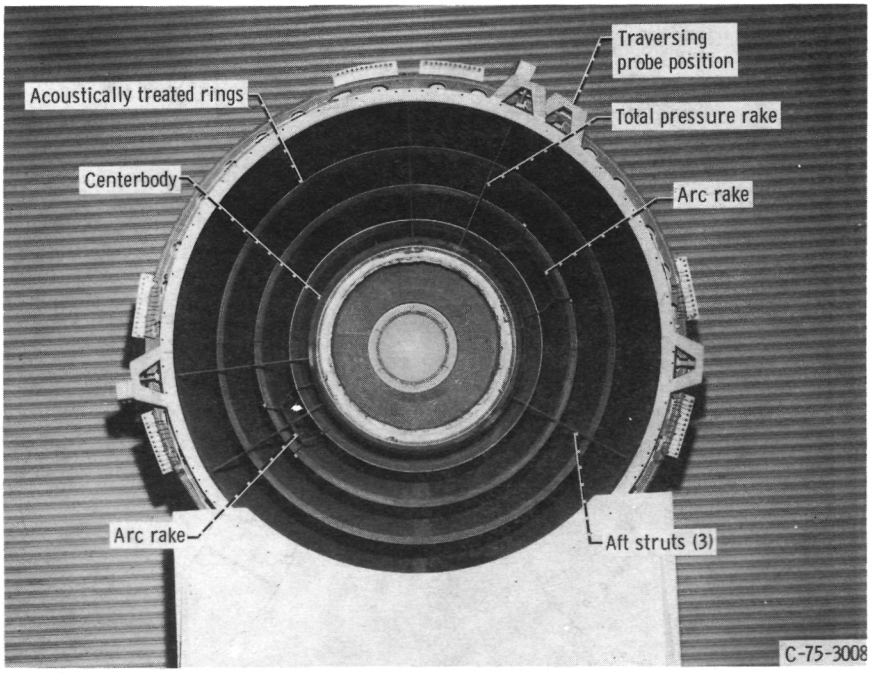

(b) Aft view.

Figure 3. - Sound suppressing inlet.

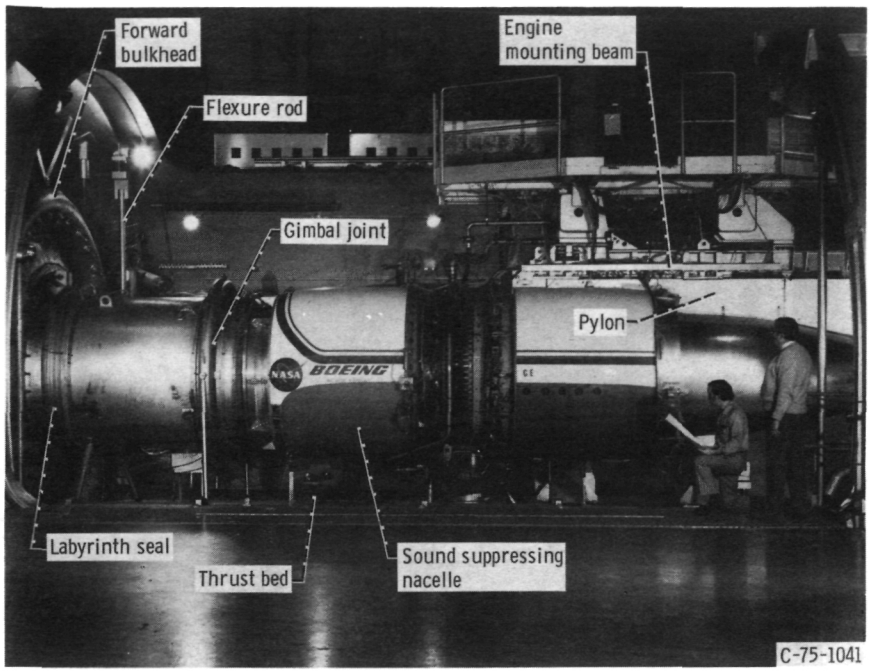

Figure 4. - Engine installation with sound suppressing nacelle.

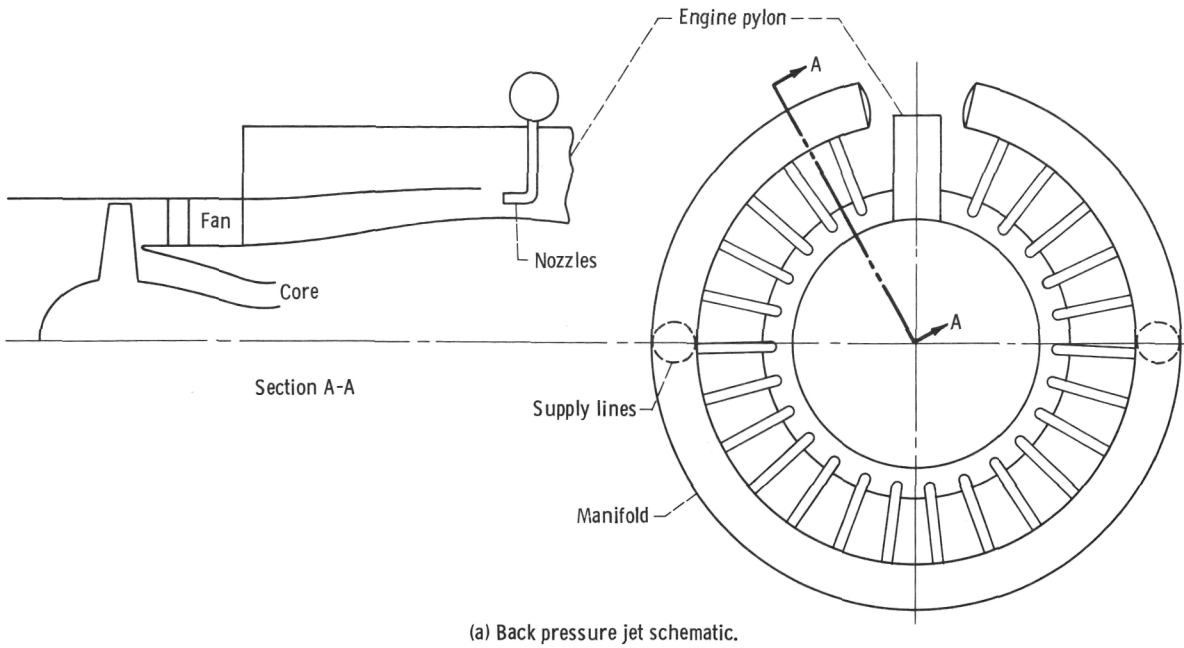

(a) Back pressure jet schematic.

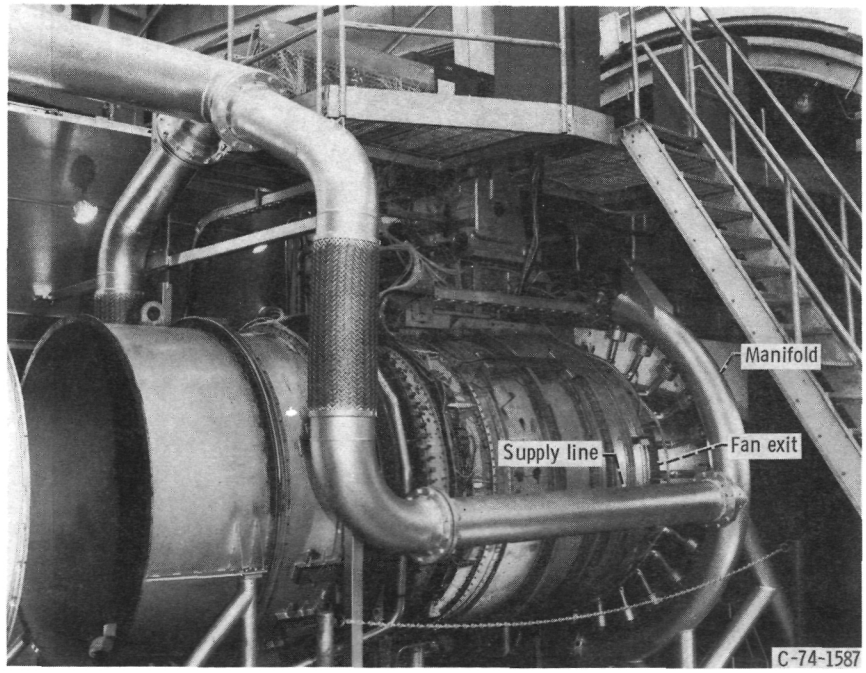

(b) Air supply system.

Figure 5. - Fan back pressure jet assembly.

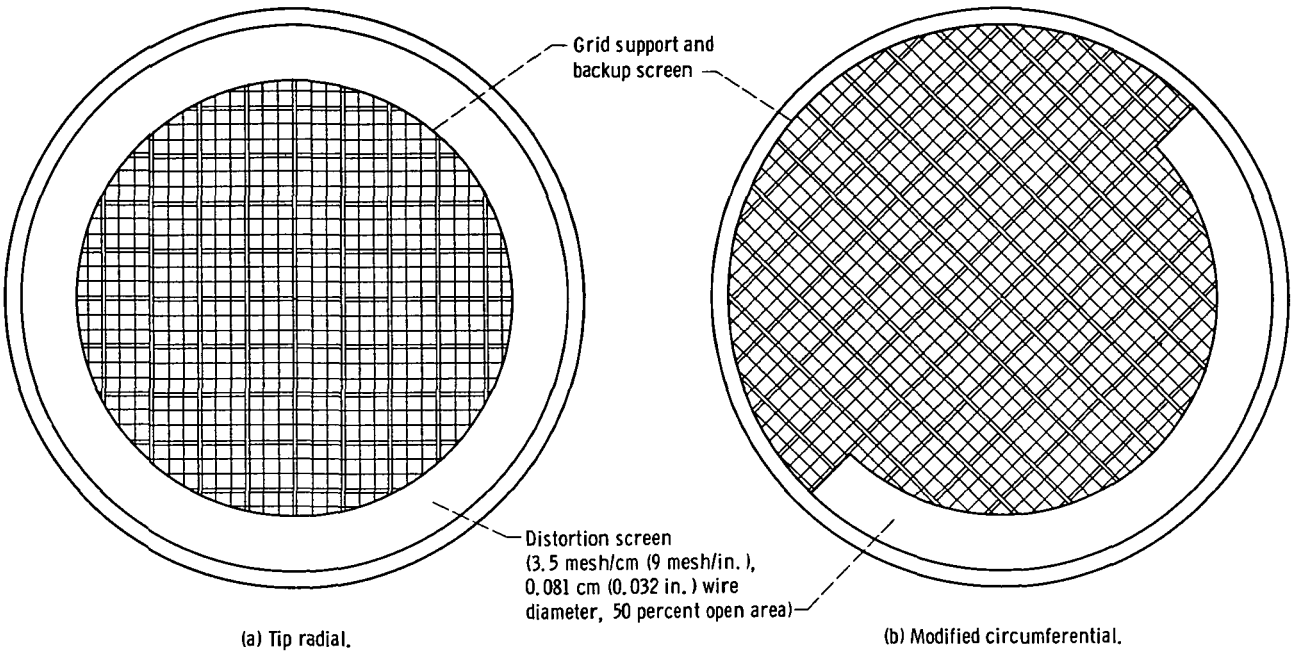

(a) Tip radial.

(b) Modified circumferential.

Figure 6. - Distortion screens used with and without sound suppressing nacelle (viewed looking downstream).

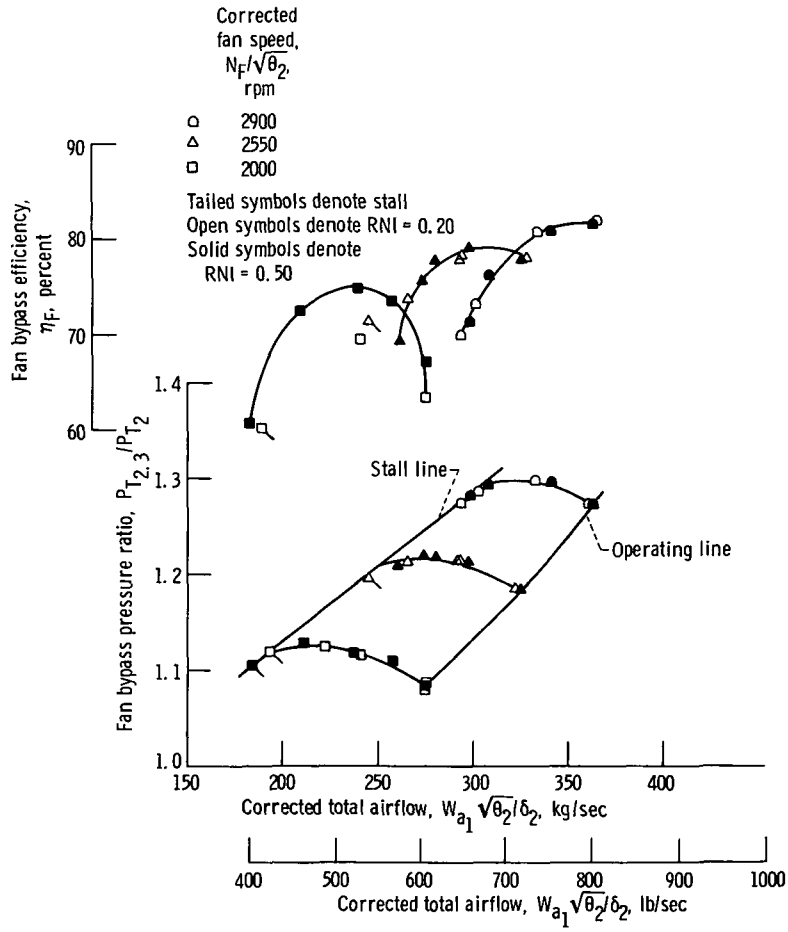

Figure 7. - Fan performance without sound-suppressing nacelle at two Reynold number indexes; flight Mach number, 0.54.

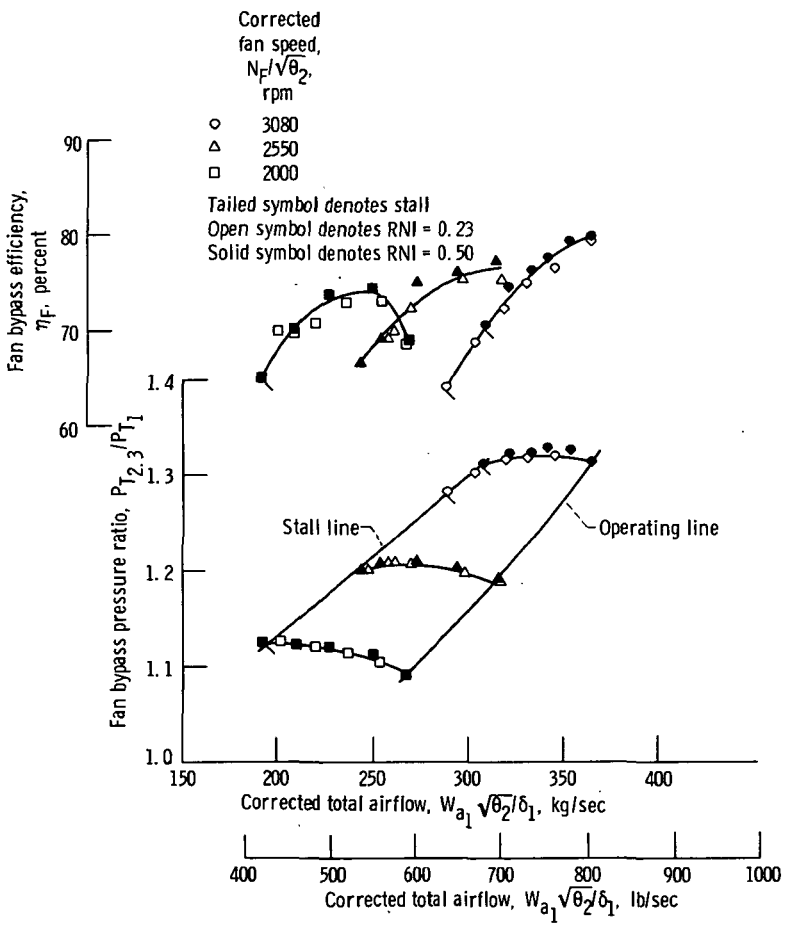

Figure 8. - Fan performance with sound suppressing nacelle at two Reynold number indexes; flight Mach number, 0.54.

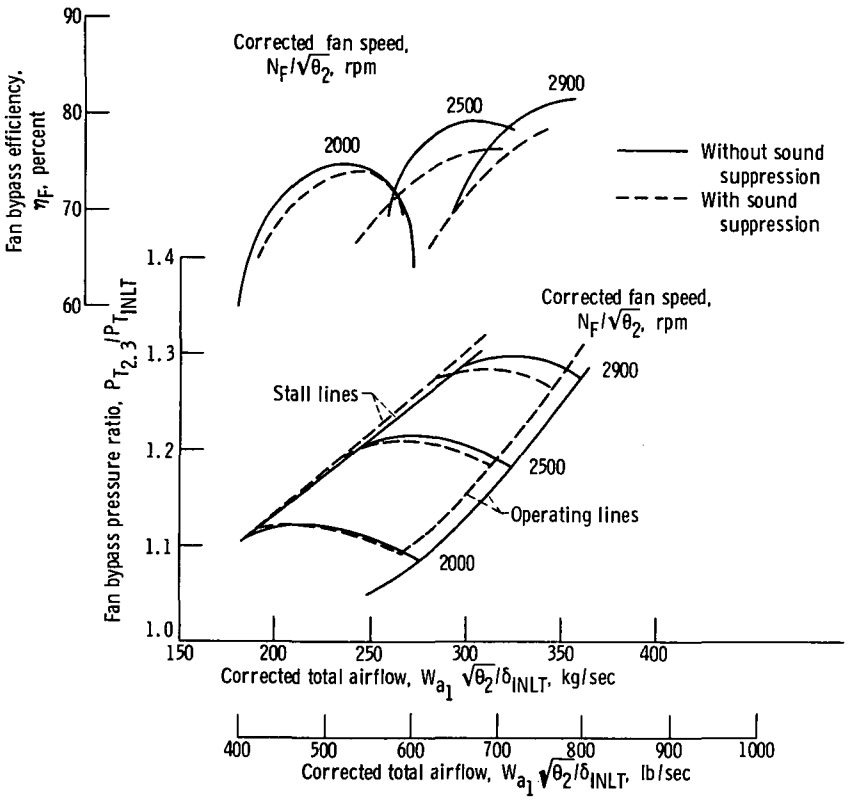

Figure 9. - Comparison of fan performance with and without sound suppressing nacelle over a range of Reynolds number indexes (0.20 to 0.50); flight Mach number, 0.54.

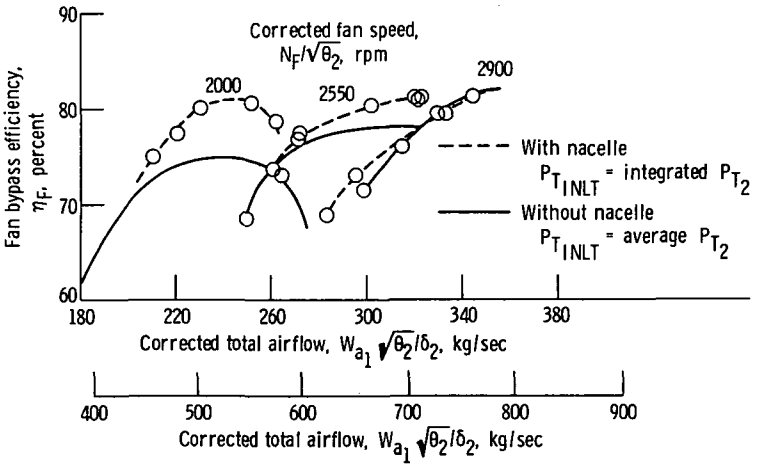

Figure 10. - Effect of sound suppressing inlet on fan bypass efficiency; Reynolds number index, 0.2; flight Mach number, 0.54.

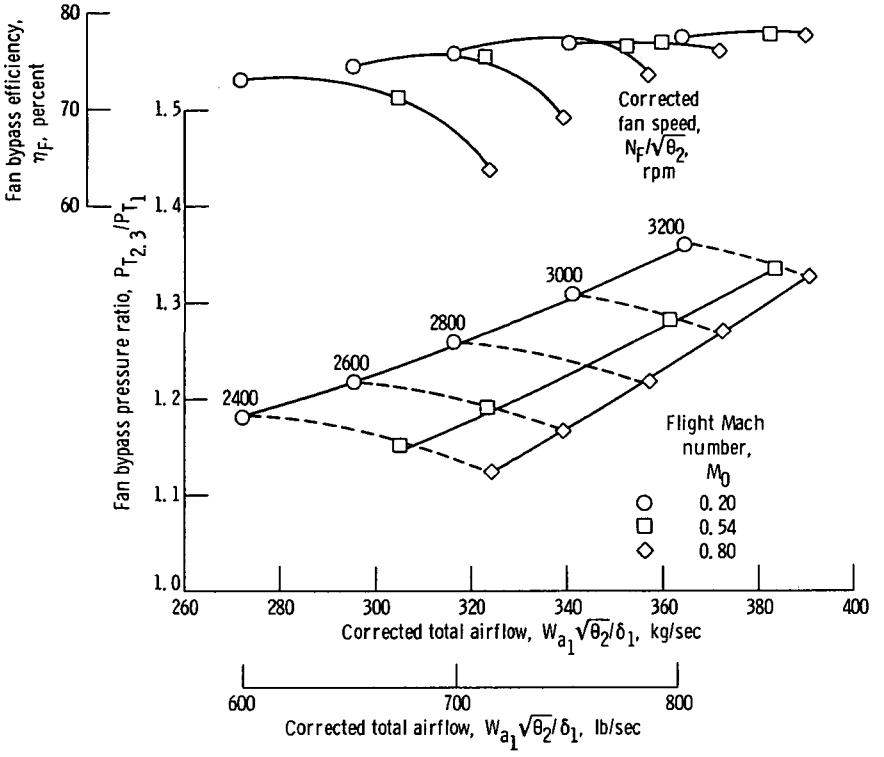

Figure 11. - Typical effect of flight Mach number on fan operating line.

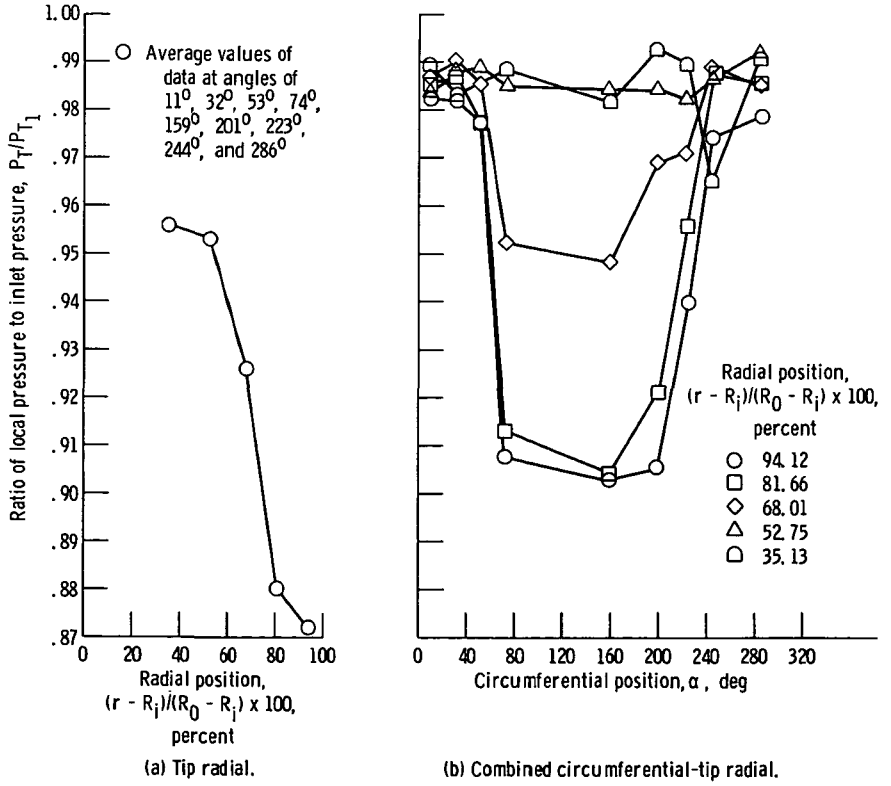

(a) Tip radial.

(b) Combined circumferential-tip radial.

Figure 12. - Typical magnitude and pattern of inlet distortions.

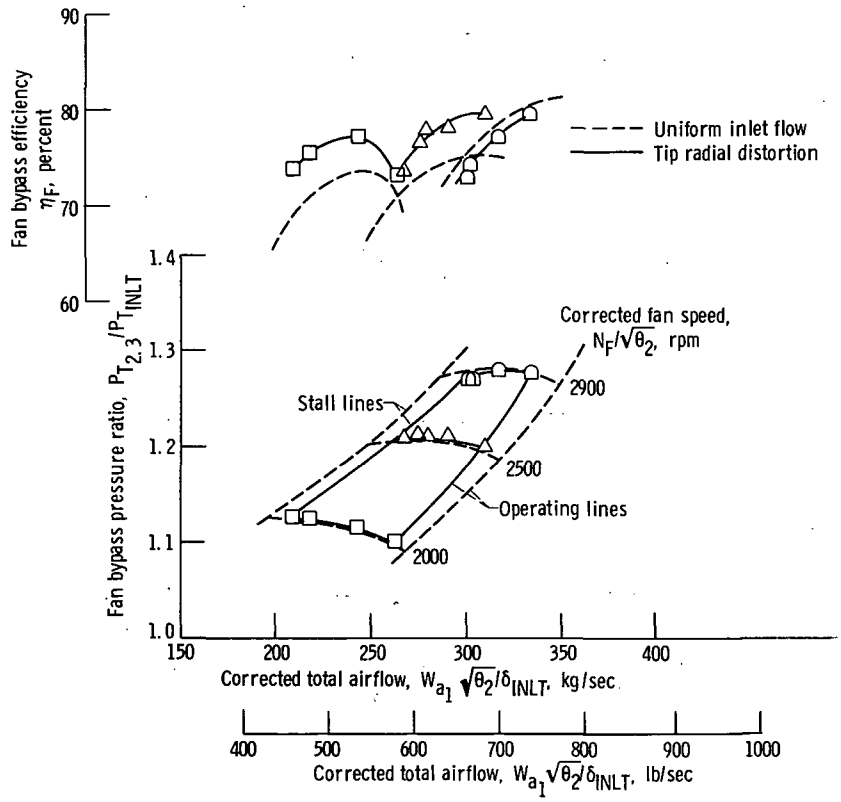

Figure 13. - Effect of tip radial distortion on fan performance with sound suppressing inlet; Reynold number index, 0.23; flight Mach number, 0.54.

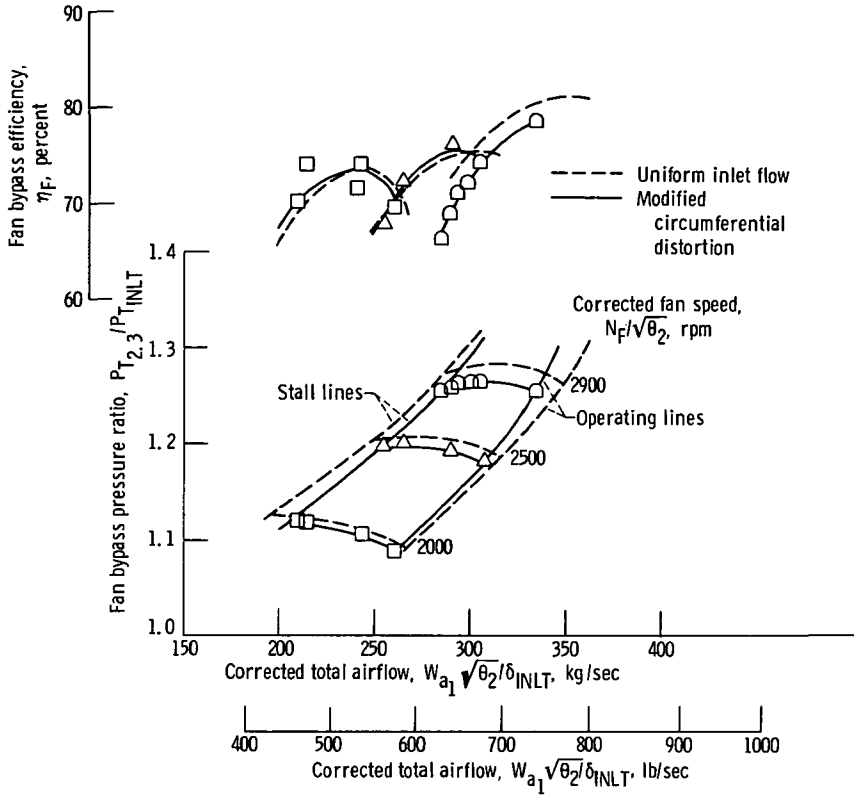

Figure 14. - Effect of modified circumferential distortion on fan performance with sound suppressing inlet; Reynolds number index, 0.23; flight Mach number, 0.54.

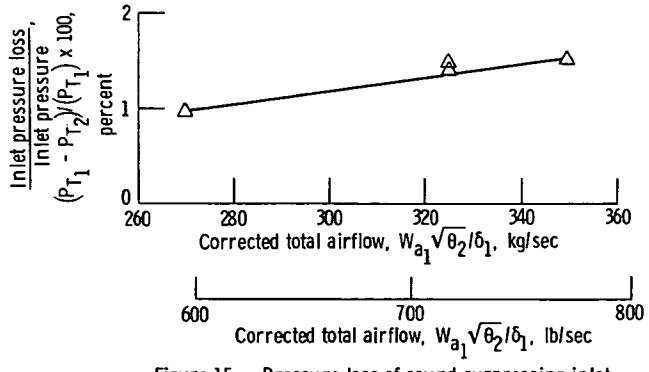

Figure 15. - Pressure loss of sound suppressing inlet.

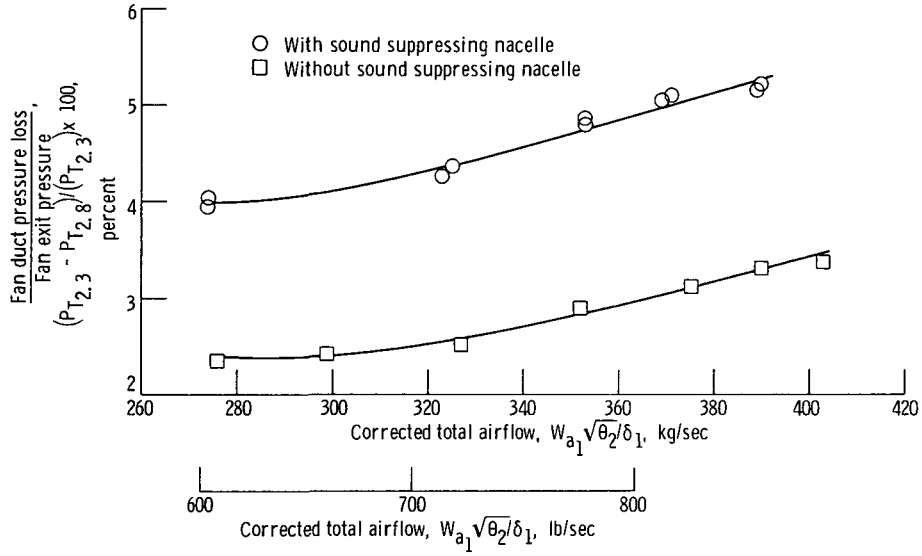

Figure 16. - Pressure loss of sound suppressing fan duct.

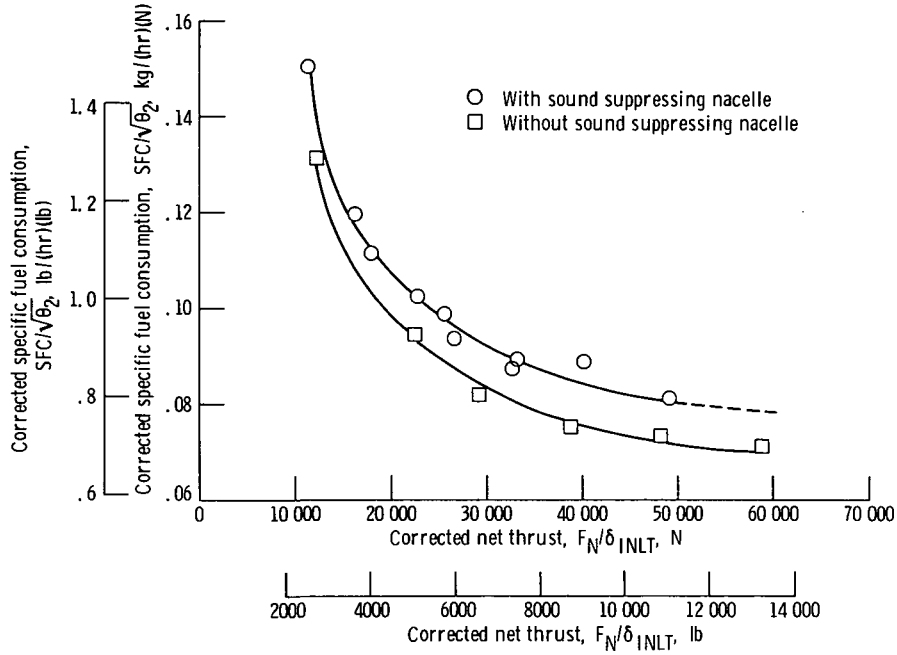

Figure 17. - Effect of sound suppressing nacelle on specific fuel consumption; Reynolds number index, 0.2; flight Mach number, 0.54.

NATIONAL AERONAUTICS AND SPACE ADMINISTRATION
WASHINGTON, D.C. 20546

OFFICIAL BUSINESS
PENALTY FOR PRIVATE USE $300

SPECIAL FOURTH-CLASS RATE BOOK

POSTAGE AND FEES PAID
NATIONAL AERONAUTICS AND SPACE ADMINISTRATION
451

U.S.MAIL

POSTMASTER: If Undeliverable (Section 158 Postal Manual) Do Not Return

"The aeronautical and space activities of the United States shall be conducted so as to contribute . . . to the expansion of human knowledge of phenomena in the atmosphere and space. The Administration shall provide for the widest practicable and appropriate dissemination of information concerning its activities and the results thereof."

—NATIONAL AERONAUTICS AND SPACE ACT OF 1958

NASA SCIENTIFIC AND TECHNICAL PUBLICATIONS

TECHNICAL REPORTS: Scientific and technical information considered important, complete, and a lasting contribution to existing knowledge.

TECHNICAL NOTES: Information less broad in scope but nevertheless of importance as a contribution to existing knowledge.

TECHNICAL MEMORANDUMS: Information receiving limited distribution because of preliminary data, security classification, or other reasons. Also includes conference proceedings with either limited or unlimited distribution.

CONTRACTOR REPORTS: Scientific and technical information generated under a NASA contract or grant and considered an important contribution to existing knowledge.

TECHNICAL TRANSLATIONS: Information published in a foreign language considered to merit NASA distribution in English.

SPECIAL PUBLICATIONS: Information derived from or of value to NASA activities. Publications include final reports of major projects, monographs, data compilations, handbooks, sourcebooks, and special bibliographies.

TECHNOLOGY UTILIZATION PUBLICATIONS: Information on technology used by NASA that may be of particular interest in commercial and other non-aerospace applications. Publications include Tech Briefs, Technology Utilization Reports and Technology Surveys.

Details on the availability of these publications may be obtained from:

SCIENTIFIC AND TECHNICAL INFORMATION OFFICE

NATIONAL AERONAUTICS AND SPACE ADMINISTRATION

Washington, D.C. 20546